ACS OMEGA

Open Access

http://pubs.acs.org/journal/acsodf

Article

Evaluating the *In Vitro* Activity and Safety of Modified LfcinB Peptides as Potential Colon Anticancer Agents: Cell Line Studies and Insect-Based Toxicity Assessments

Karen J. Cárdenas-Martínez, Andrea C. Barragán-Cárdenas, Manuela de la Rosa-Arbeláez, Claudia M. Parra-Giraldo, Alejandra Ochoa-Zarzosa, Joel E. Lopez-Meza, Zuly J. Rivera-Monroy, Ricardo Fierro-Medina, and Javier E. García-Castañeda*

Cite This: *ACS Omega* 2023, 8, 37948−37957

Read Online

ACCESS | Metrics & More | Article Recommendations | Supporting Information

ABSTRACT: Anticancer peptides are increasingly being considered as alternative treatments for cancer due to their potency, selectivity, and low toxicity. Previously, the peptide LfcinB $(21-25)_{Pal}$ showed *in vitro* anticancer effects against the Caco-2 colon cancer cell line (half-maximal inhibitory concentration (IC_{50}): 86 μM). In this study, we developed modifications to the peptide sequence to increase its anticancer activity. Sequence modifications were made such as the inclusion of amino hexanoic acid (Ahx), N-terminal biotinylation, acetylation, and substitutions of Orn for Arg and/or D-Arg by L-Arg. The molecules were synthesized using manual solid-phase peptide synthesis (SPPS), and their synthetic feasibility (SAScore) ranged from 6.2 to 7.6. The chromatographic purities of the synthesized peptides were greater than 89%. We found that Ahx-RWQWRWQWR and RWQWRWQW-Orn showed activity against both Caco-2 and HT-29 cell lines and decreased IC_{50} values by approx. 50% in Caco-2 cells (IC_{50}: 40 μM) when compared to the parent peptide RWQWRWQWR. Moreover, the modified peptides demonstrated lower hemolytic effects, with values <10% at 200 μg/mL. Toxicity was assessed using the Galleria mellonella model and the half-maximal lethal dose (LD_{50}) for the best peptides was >100 mg/kg, indicating that their toxicity is classified as moderately toxic or lower. In contrast, cisplatin showed an LD_{50} of 13 mg/Kg. The designed anticancer peptides presented good *in vitro* activity and low toxicity, making them promising molecules for future drug development studies.

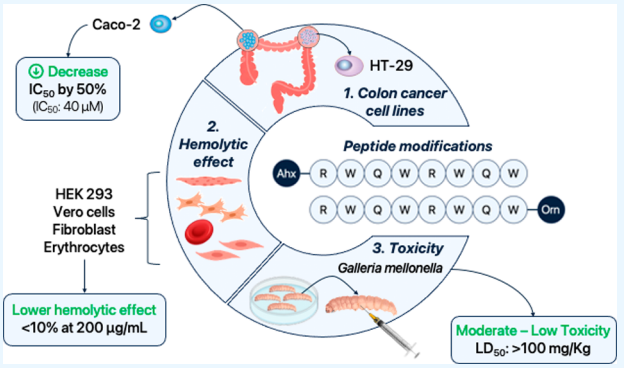

INTRODUCTION

The development of selective cancer treatments remains a challenge despite significant research efforts. Current novel therapies are costly, and the mortality rate remains high. Additionally, chemotherapy resistance has emerged as a new challenge in the fight against cancer, highlighting the need for designing drugs beyond traditional molecules.[1]

Colon cancer incidence has decreased over the years; however, it is still a leading cause of death.[2] Furthermore, the prevalence of this cancer has shifted from older patients to the younger population (<50 years old), an age group where screening is limited.[3] Additionally, cases have increased in middle- and low-income countries,[4] raising concerns about the efficacy of early detection and treatment options, particularly at more advanced stages.[5,6]

Therapies focused on exploiting the differences between cancer cells and normal cells could potentially increase selectivity and decrease side effects. Normal cells typically exhibit a zwitterionic nature, resulting in an overall neutral charge. They possess phosphatidylcholine and sphingomyelin on their external surface. In contrast, cancer cells predominantly display phosphatidylserine and phosphatidylethanolamine, contributing to a negative charge on their membrane. Also, cancer cells exhibit other molecules such as *O*-glycosylated mucins, sialylated gangliosides, and certain metabolic features that contribute to their negative charge.[7,8] These alterations in phospholipids have been observed in human colorectal cancer cells, with cancer cells showing elevated expression of phosphatidylcholine and phosphatidylethanolamine.[9] Furthermore, the presence of sialic acid in the membrane is associated with tumorigenesis and cancer cell migration.[10]

Received: May 17, 2023
Accepted: August 15, 2023
Published: October 4, 2023

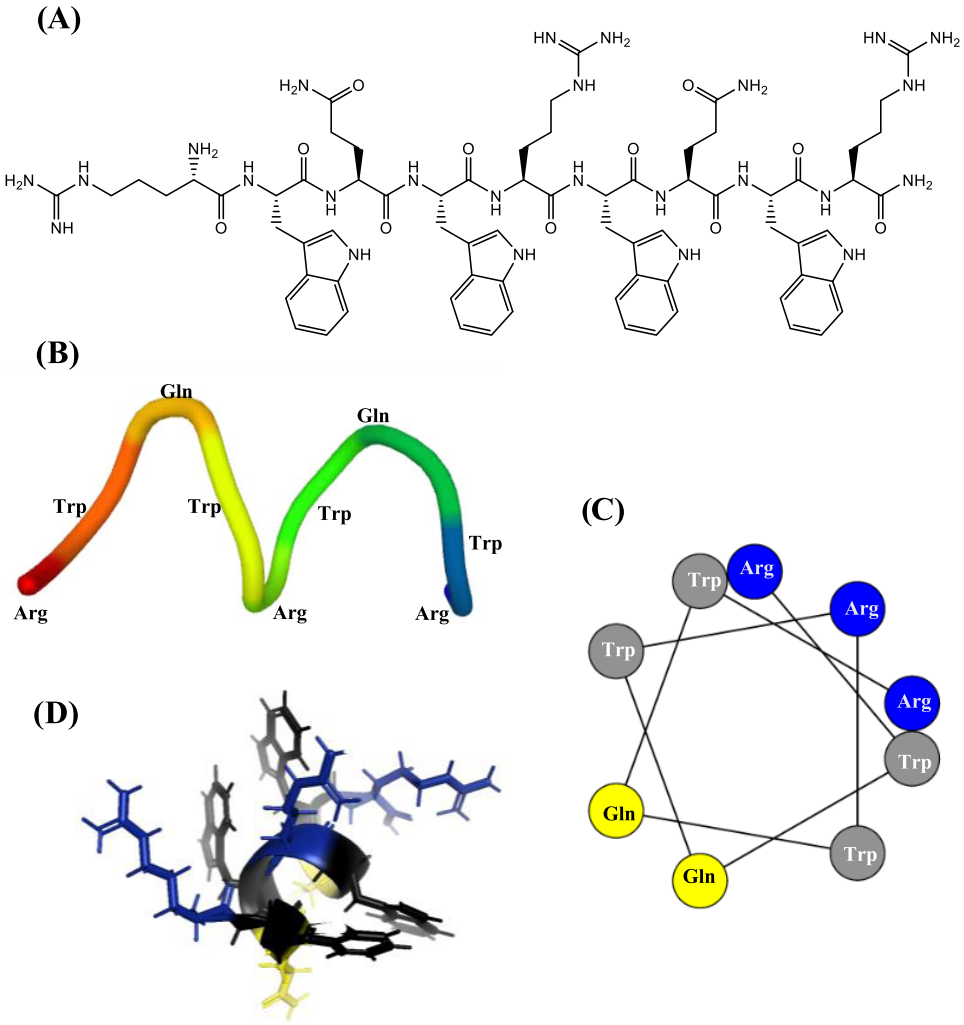

Figure 1. Structural characteristics of the [Pal] peptide. (A) Chemical structure and (B) helical structure from the PEP-FOLD server.[24,25] (C) Helical wheel structure. The heatmap was plotted by https://www.bioinformatics.com.cn/en, a free online platform for data analysis and visualization. (D) Maestro−Schrödinger's projection.

This negative charge present on cancer cell membranes serves as a starting point for selective electrostatic recognition with cationic molecules, such as cationic peptides, which are part of some called anticancer peptides (ACPs). Similarly, it has been demonstrated that alterations in lipid-associated pathways in cancer cells result in the presence of cholesterol on their membranes, making them more fluid.[11,12] This increased fluidity facilitates their internalization of anticancer peptides. Furthermore, the presence of microvilli on the cancer cell surface membrane leads to an increased surface area, allowing for enhanced interactions with peptides.[7,13] Following the initial electrostatic recognition, peptides can exert their activity, which could include oncolytic, target-mediated, or pro-apoptotic activities, among others.[14]

ACPs are recognized as promising alternative strategies in the fight against cancer owing to their selectivity, low toxicity, and efficacy. ACPs typically possess cationic charges due to the presence of arginine (Arg), lysine (Lys), and histidine (His), as well as hydrophobic amino acids, which enable an optimal balance for cell permeability. However, the widespread use of peptides faces challenges due to certain disadvantages, such as low stability, which can result in reduced *in vivo* effectiveness.[15] Nonetheless, the advantages outweigh these disadvantages, as evidenced by the steadily increasing number of peptides available in the market.[7]

Among the ACPs, the palindromic peptide derived from bovine lactoferricin (LfcinB), RWQWRWQWR [Pal], has demonstrated antifungal, antibacterial, and anticancer effects against breast and colon cancer cell lines.[16,17] In previous studies, we investigated the impact of Arg/Lys changes on the antimicrobial activity of the molecule, revealing that the Lys analogue exhibited similar antibacterial activity and lower hemolytic activity.[18] We also explored the modification of net charge quantity and its effect on breast cancer cell lines, finding that the effect was not solely dependent on the charge but also on its location (N or C terminal).[19] This observation drew our attention to specific amino acid changes. In this study, we report the enhanced anticancer activity of the palindromic sequence through modifications aimed at medicinal chemistry optimization. Additionally, we utilized the Galleria mellonella model to assess toxicity.

RESULTS AND DISCUSSION

The palindromic peptide [Pal] has previously demonstrated anticancer activity against the Caco-2 colon cancer cell line. This peptide has a palindromic sequence consisting of nine

https://doi.org/10.1021/acsomega.3c03455
ACS Omega 2023, 8, 37948−37957

Table 1. Characterization of the Obtained Peptides

		RP-HPLC				
code	sequence	t_R (min)	purity (%)	expected mass	obtained mass	SAscore
[Pal]	RWQWRWQWR	6.4	99	1485.76	1486.14	6.3
Ahx-[Pal]	**Ahx**-RWQWRWQWR	6.3	99	1599.88	1598.82	6.6
Biotin-Ahx-[Pal]	**Biotin-Ahx**-RWQWRWQWR	6.9	91	1824.93	1824.91	7.6
^{1}[^{d}R][Pal]	^{d}**R**WQWRWQWR	6.4	89	1485.76	1485.74	6.2
^{1}[Orn] [Pal]	**Orn**-WQWRWQWR	6.4	95	1443.74	1443.74	6.2
^{5}[Orn] [Pal]	RWQW-**Orn**-WQWR	6.4	96	1443.74	1444.61	6.2
^{9}[Orn] [Pal]	RWQWRWQW-**Orn**	6.3	94	1443.74	1443.72	6.2
^{1}[^{d}R] ^{5}[Orn] [Pal]	^{d}**R**WQW-**Orn**-WQWR	6.3	95	1443.74	1443.74	6.2
CH_3CO-Ahx-[Pal]	**CH_3-CO-Ahx**-RWQWRWQWR	6.6	98	1640.86	1640.84	6.7

residues. The circular dichroism spectra showed that in solution, this peptide adopts a random coil secondary structure.[17] It is currently unclear whether it adopts an α helical conformation upon contact with the cell, and future biophysical studies are planned to address this matter. However, it has been suggested that anticancer peptides acquire helical conformation when they interact with curved hydrophobic surfaces such as small unilamellar vesicles (SUVs) or sodium dodecyl sulfate (SDS) micelles. Peptides have shown varying degrees of helicity in different environments, but they consistently exhibit a higher tendency to form an α-helical structure in anionic environments (e.g., cancer cell surface),[20−22] which must be evaluated and is beyond the scope of this study. To investigate the effect of changes in the palindromic sequence on the helical wheel representation of these peptides, we compared the helical wheel representations of the palindromic peptide and its analogues. This prediction tool can be used to describe the orientation of side chains of amphipathic sequences such as LfcinB and analogous sequences. For this type of sequence, two possible behaviors have been described: (i) random coil peptides may adopt secondary structure conformations (α helix) when interacting with the cell membrane and (ii) it has been suggested that LfcinB forms aggregates as a prerequisite for interacting with the cell membrane, these aggregates possibly result from the interaction between the nonpolar faces of the sequence. From this, it is intended to establish whether the changes of amino acids in the palindromic sequence affect the polarity of the faces using the helical conformation as a basis.[23] In addition, helical prediction serves as a valuable starting point for the rational design and engineering of peptides. It facilitates the identification of specific regions within the peptide that can guide a systematic and informed design approach.

The helical wheel representation (of the possible helical structure) reveals that the peptide possesses a well-defined polar cationic side, which is flanked by two hydrophobic regions containing tryptophan (Trp) residues and one noncharged polar side composed of glutamine (Gln) (Figure 1C). Previous studies in breast cancer have shown that substituting any residue with Ala results in a loss of activity,[17] underscoring the importance of each residue in the anticancer activity.

In the structure (Figure 1), all of the Arg residues are positioned on one face, which could facilitate the initial electrostatic interaction with the cell membrane. Subsequently, the presence of Trp residues may favor hydrophobic interactions with the membrane lipid bilayer. The precise location of these residues in a structurally well-defined manner is responsible for the amphipathic properties of the peptide.

To enhance the anticancer activity of the palindromic peptide, we introduced modifications while retaining the previously mentioned structural features. The modifications encompassed the following: N-terminal amino hexanoic (Ahx) incorporation or biotinylation, acetylation, and substitutions of L-Arg by D-Arg (^{d}R) and/or ornithine (Orn). These modifications were carefully designed to preserve the cationic and hydrophobic features of the peptide while improving its selective anticancer activity. The results suggest that some modified versions of the palindromic peptide hold promise for advancing the development of more potent and targeted anticancer therapies.

First, the synthetic *in silico* feasibility of the peptides was determined using the ADMETLab 2.0 platform[26] and SAScore.[27] These results correlate with the experimental findings, which revealed significant challenges when dealing with longer sequences. The results ranged from 6.2 to 7.6 on a scale of 1 to 10, with 10 indicating the most challenging molecule to synthesize. These peptides consist of short linear motifs, making Fmoc solid-phase peptide synthesis (Fmoc/tBu-SPPS) generally straightforward. Therefore, this platform was valuable in assessing the synthetic process's feasibility and ranking its efficiency.[27] In this case, the synthesis was directly correlated with the peptide sequence's length (Table 1 and Figure S11).

All peptides were successfully synthesized and characterized, achieving chromatographic purities above 89%. The mass analysis confirmed that the observed values matched the expected values. Notably, none of the modifications significantly altered the peptides' retention time, suggesting minimal changes in their hydrophobic properties.

The molecules were evaluated for their anticancer activity against colon cancer cell lines HT-29 and Caco-2 (Table 2 and Figures S10 and S12). Cell viability assays were performed, revealing that the HT-29 cell line exhibited higher resistance to the treatment. The first approach to increase the potency was to include biotin. This choice was based on the presence of a higher quantity of vitamin receptors on the surface of some cancer cells, potentially increasing the cell permeability of the molecules.[28] Additionally, the biotinylated peptide could serve as a probe for analyzing the mechanism of action of the peptide.[29]

For the design of this modified molecule, amino hexanoic acid (Ahx) was used as a linker/spacer.[31] However, biotinylation resulted in the complete loss of activity against both cancer cell lines. To understand this effect, the theoretical value of log *P* was examined. It was observed that the presence of biotin significantly modified this property compared to the parent peptides, rendering the molecule more lipophilic.

https://doi.org/10.1021/acsomega.3c03455
ACS Omega 2023, 8, 37948−37957

Table 2. Log *P* of the Molecule Determined in ADMETLab 2.0 Software[30] and Inhibitory Concentration (IC_{50}) of Peptides against Colon Cancer Cell Lines

code	log *P*	IC_{50} (μM/μg/mL)	
		HT-29	Caco-2
[Pal]	0.24	100/149	86/127
Ahx-[Pal]	−0.64	119/190	40/65
Biotin-Ahx-[Pal]	1.21	>110/>200	>110/>200
CH_3CO-Ahx-[Pal]	0.84	>122/>200	31/52
^{1}[^{d}R][Pal]	−0.05	>135/>200	105/155
^{1}[Orn] [Pal]	0.25	>138/>200	91/132
^{5}[Orn] [Pal]	0.47	>138/>200	64/92
^{9}[Orn] [Pal]	0.25	109/157.5	40/58
^{1}[^{d}R] ^{5}[Orn] [Pal]	−0.92	>138/>200	109/158

Previous reports have indicated that increasing the lipophilicity of ACPs, such as through the use of lipids or hydrophobic amino acids, can enhance their activity.[32,33] However, the ideal lipophilicity value for optimal activity remains undefined. Further investigations are required to elucidate the precise mechanisms underlying the relationship between lipophilicity and the activity of these anticancer peptides.

Predicting log *P* in peptides can be challenging and less straightforward compared to small molecules. Moreover, certain software tools may have limitations, such as the inability to handle long peptide sequences or unnatural residues, which can hinder accurate log *P* prediction. In this study, log *P* calculations were performed using the ADMETLab platform. The log *P* value, as described by this algorithm, represents the logarithm of the molar concentration. According to this platform, molecules with log *P* values ranging from 0 to 3 are considered druggable.[26] While log *P* serves as an initial approach to understanding the physicochemical characteristics of the peptides in this study.

The peptide containing only the Ahx residue was synthesized to assess whether the loss of activity was attributable to the linker inclusion. Interestingly, the cytotoxic activity against HT-29 was maintained, while the effect on Caco-2 cells was enhanced by 2-fold. This discrepancy in activity suggests distinct interaction patterns between the peptides and the two cell lines. Despite Ahx being a hydrophobic amino acid itself,[31] in the *in silico* analysis, its presence in the peptide led to a decrease in overall lipophilicity, possibly due to changes in the arrangement of the molecule by changing intermolecular interactions. Nonetheless, the inclusion of Ahx is unlikely to interfere with the interaction between the peptide's cationic charges and the cell membrane, assuming that the peptides adopt an α helical conformation (Figure 2A).

To further investigate the observed effect, the acetylated moiety was introduced to determine if it was solely responsible for the loss of activity rather than the voluminosity of biotin. Surprisingly, the activity against HT-29 cells was completely abolished at the evaluated concentrations, while it increased against Caco-2 cells. The results showed that peptides Ahx-[Pal] and CH_3CO-Ahx-[Pal] presented higher anticancer activity in Caco-2 cells than in HT-29 cells.

To explore the impact of chirality on the activity of the molecules, we investigated the effect of changing the chirality of the N-terminal Arg residue in the parent sequence. This modification had a significant effect on the peptide's effectiveness, leading to a complete loss of activity in the HT-29 cell line and a decrease in activity in Caco-2 cells. This suggests that the positioning of the amine group is also crucial for the peptide's activity. Notably, this modification did not result in any significant change in the molecule's polarity. This result suggests that the peptide−cell interaction could be conformational in nature.

Considering the significant influence of the peptide's cationic charge on its activity, we further examined whether modifying the amino acid responsible for this effect, Arg, could have implications. To explore this, sequential changes of Arg/Orn were introduced. These modifications were guided by the knowledge that while Arg is critical for selective membrane recognition, it may also impact the peptide's selectivity.[34] Additionally, recognizing that both Arg and Lys are susceptible to proteolytic degradation, we opted to use Orn, an unnatural amino acid, for these modifications.

At this point, it is interesting to note that when analyzing the chemical structure of the cationic residues that positively influenced the activity of the peptides (Figure 3), there were differences in the nature of the cationic charge (when comparing the guanidinium group of Arg to the amino group of Orn and Ahx). It is currently recognized that the guanidinium groups exert stronger interactions with the cell membrane;[18,35] however, the variations in the number of carbon atoms in the side chain of Orn and Ahx, could

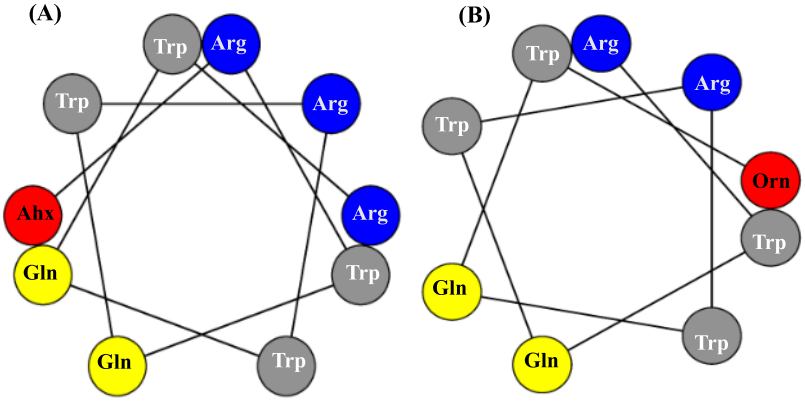

Figure 2. Helical wheel conformation prediction of peptides (A) Ahx-[Pal] and (B) ^{9}[Orn] [Pal]. The heatmap was plotted by https://www.bioinformatics.com.cn/en, a free online platform for data analysis and visualization.

https://doi.org/10.1021/acsomega.3c03455
ACS Omega 2023, 8, 37948−37957

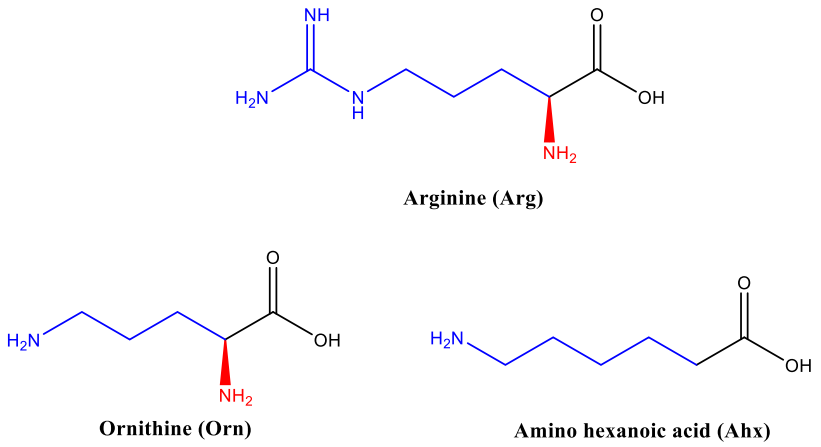

Figure 3. Structure of the residues: arginine, ornithine, and amino hexanoic acid.

potentially impact the distance of intermolecular interactions occurring with the membrane.

In the original sequence, there were three Arg residues and changes at positions 1 and 5 resulted in a loss of activity, even though the palindromic nature of the molecule was maintained, as observed with the ^{5}[Orn] [Pal] variant. Interestingly, one of the modifications, ^{9}[Orn] [Pal] (Figure 2B), preserved the activity against HT-29 cells and exhibited a 2-fold increase in potency against the Caco-2 cell line. This finding highlights the potential importance of future modifications at this specific position. Moreover, upon contact with the cells for 2 h, morphological changes were observed, including cell shrinkage and membrane blebbing, which are characteristic apoptotic changes (Figure 4).

After studying the effect against colon cancer cells, we analyzed the cytotoxicity against control cell lines; as an initial evaluation of the selectivity, we tested the effect over human fibroblasts, HEK-293, and Vero cells (Table 3 and Figure 5). Over the three cell lines, Vero cells were the most susceptible to the effect of the peptide. Vero cells can be used as a model for *in vitro* toxicity due to their high use and susceptibility.[36,37] The modified peptides showed better selectivity, especially when compared to Caco-2 cells, which means that in this case, the modifications improved the selectivity at the IC_{50} concentration. However, at the maximum tested concentration, there were no significant differences. In contrast, both modified peptides lost selectivity against fibroblast, and there were no significant differences in the effect over HEK-293, while micrographs show cell damage at 200 μg/mL.

None of the modified peptides exhibited a significant hemolytic effect at the highest concentration tested, indicating a favorable safety profile for these peptides. This observation aligns with the *in silico* predictions obtained from the HAPPENN platform, which assigned a normalized sigmoid score of 0.033 for the hemolytic potential of the parent peptide [Pal]. The scoring system ranges from 0 to 1, with 1 representing the highest likelihood of hemolysis.[38] This positive correlation between experimental and *in silico* findings facilitates the screening of molecules during hit studies, enhancing the efficiency of the screening process. However, the HAPPENN platform currently lacks the capability to analyze peptides with unnatural residues, which could be needed for further analysis.

We also wanted to predict the protein plasma binding (% PPB) by using ADMETLab 2.0, as some other known

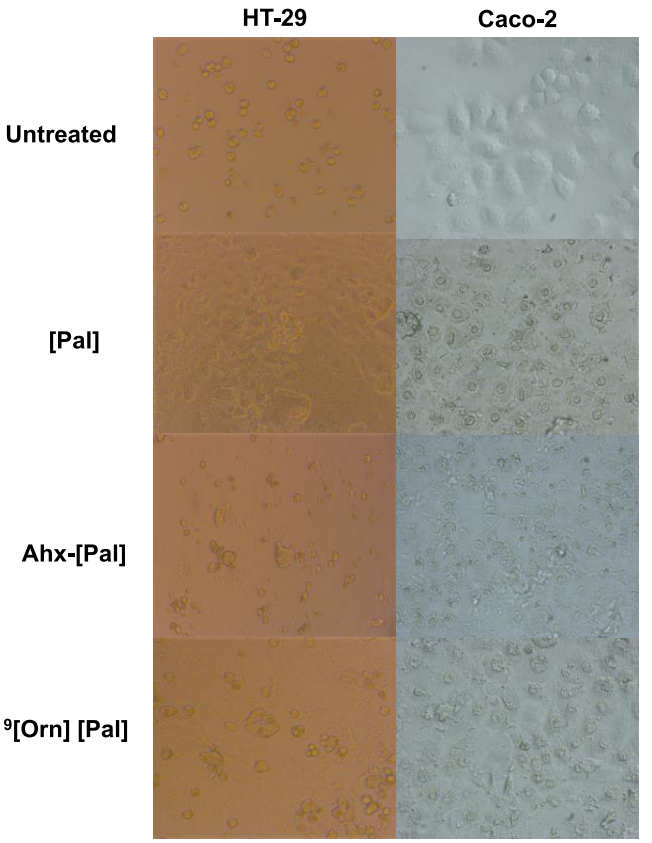

Figure 4. Micrography of HT-29 and Caco-2 colon cancer cells treated with peptides at the maximum peptide concentration (200 μg/mL) using an AxioCam ICc1 camera (scale bar: 100 μm).

platforms are not designed for such large molecules; however, further studies need to be done to corroborate these results. All three molecules presented a %PPB ranging between 66.7 and 76.1. This moderate binding could indicate useful insights into stability and distribution, which is known to be low for linear peptides.[39]

We proceeded to assess the toxicity of the most promising peptides using the Galleria mellonella toxicity model. For this evaluation, we selected a maximum concentration of 100 mg/Kg and conducted acute toxicity testing over a period of 10 days (Figure 6). Interestingly, none of the peptides demonstrated significant toxicity, in contrast to the control

https://doi.org/10.1021/acsomega.3c03455
ACS Omega 2023, 8, 37948−37957

Table 3. Cytotoxic Activity of Peptides against Control Cells[a]

	CC_{50} (μM/μg/mL)		
cell line	[Pal]	Ahx-[Pal]	^{9}[Orn] [Pal]
HEK-293	68/101	86/132	51/74
Vero	21/31	40/64	46/67
fibroblasts	>134/>200	98/157	55/79
hemolysis (%)*	13.2	7.7	6.6
Selectivity Index			
HEK-293/HT-29	0.7	0.7	0.5
HEK-293/Caco-2	0.8	2.2	1.3
Vero/HT-29	0.2	0.3	0.4
Vero/Caco-2	0.2	1.0	1.2
fibroblasts/HT-29	>2.0	0.8	0.5
fibroblasts/Caco-2	>2.5	2.5	1.4
erythrocytes/HT-29	1.3	>1.1	>1.3
erythrocytes/CaCo-2	1.6	>3.1	>3.4

[a]Hemolytic activity was evaluated at 200 μg/mL*. The selectivity index (SI) was defined as CC_{50}/IC_{50}, and in erythrocytes, hemolysis10%/IC_{50}.

cisplatin group, which exhibited a mortality rate of 93% (Figure 6A). Furthermore, we specifically analyzed the modified peptide ^{9}[Orn] [Pal] at concentrations ranging from 20−100 mg/Kg (Figure 6B). Notably, this peptide did not show any significant toxicity.

When making a similar analysis with cisplatin, we found dose-dependent concentrations (10−100 mg/kg), which presented complete mortality at 40 mg/kg (Figure 6C). By linearizing the obtained results within the range of 10−40 mg/kg, we determined the LD_{50} for cisplatin to be 13 mg/Kg ($y = 93.75x - 55.21$; $r^2 = 0{,}74$), a value that partially correlates with previous studies on Galleria (60% of mortality at 33 mg/kg[40]) and mice (15.3 ± 1.6 mg/kg[41]). Interestingly, after 30 min of treatment, the larvae exhibited visible muscle contractions throughout their entire bodies in the form of tremors. These tremors could potentially be attributed to the locomotor effects resulting from the well-established neurotoxicity of cisplatin.[41]

This correlation, while adhering to the principles of 3Rs (replacement, reduction, and refinement), makes this model valuable to provide insights into the potential toxicity of compounds, useful in the preliminary toxicity assessments. These results underscore the potential of the tested peptides as safer alternatives to traditional chemotherapy drugs, such as cisplatin, with reduced likelihoods of adverse effects.

Due to the possibility of colon cancer metastasizing to other organs, including the prostate,[42,43] we conducted an analysis of the peptides' effect over the Du-145 cell line (Table 4 and Figure 7). This study represents the first report on the effect of the parent peptide on a prostate cancer cell line. Prior to this, the peptide had demonstrated effects over breast, colon, and oral cancer cell lines, expanding the spectrum effect of its anticancer activity. Interestingly, we noticed that there was a complete loss in activity when the Ahx was added; therefore, we identified the parent peptide and ^{9}[Orn] [Pal] as the most promising molecules based on their potential therapeutic efficacy.

CONCLUSIONS

A series of modifications were made to the palindromic peptide [Pal] derived from the bovine lactoferricin sequence. Within this study, we found that the parent peptide and the modification ^{9}[Orn] [Pal] presented activity against the HT-29 and Caco-2 colon cancer cell lines and Du-145 prostate cancer cell line. The absence of significant hemolytic effects and the

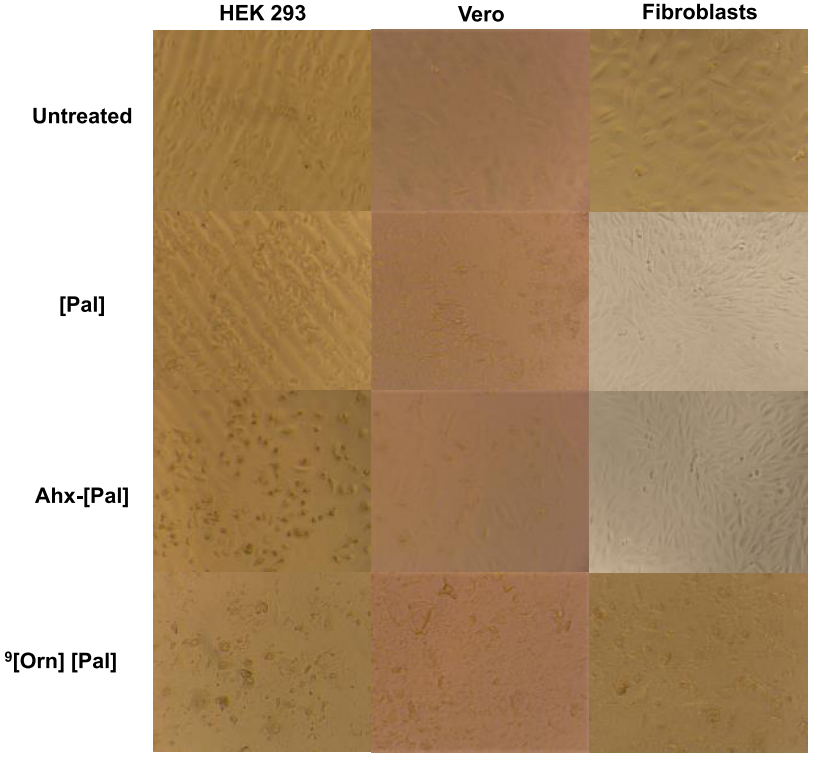

Figure 5. Micrography of fibroblast, HEK-293, and Vero cells treated with peptides at the maximum peptide concentration (200 μg/mL) using an AxioCam ICc1 camera (Scale bar: 100 μm).

https://doi.org/10.1021/acsomega.3c03455
ACS Omega 2023, 8, 37948−37957

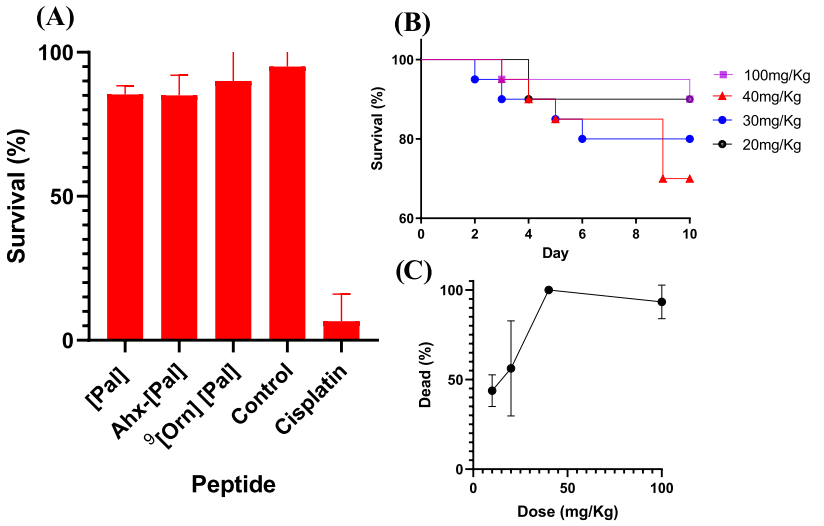

Figure 6. Galleria mellonella toxicity test. (A) Survival percentage at a dose of 100 mg/kg; there is not a significant difference between the peptides and control. (B) Kaplan–Meyer curve at different concentrations for peptide ^{9}[Orn] [Pal]. There is not a significant difference among peptide groups (n = 2). (C) Curve dose–response for cisplatin.

Table 4. Inhibitory Concentration (IC_{50}) of Peptides against the Du-145 Cancer Cell Line

code	IC_{50} (μM/μg/mL) Du-145
[Pal]	40/60
Ahx-[Pal]	>200
^{9}[Orn] [Pal]	62/89

favorable safety profiles observed in the Galleria mellonella model provide promising evidence for the potential clinical applications of these peptides. Our findings underscore the potential of the peptides as safer alternatives to traditional chemotherapy drugs like cisplatin (LD_{50} in Galleria mellonella of 13 mg/kg).

METHODOLOGY

Synthesis of the Peptides. The peptides were synthesized using manual solid-phase peptide synthesis (SPPS-Fmoc/tBu). Briefly, Rink amide resin (0.46 meq/g) was swelled with *N*,*N*-dimethylformamide (DMF) for 2 h, followed by two cycles of deprotections through treatment with 2,5% 4-methylpiperidine in DMF and then washed with DMF and DCM. For the coupling reaction, five equivalents of excess were used, Fmoc-amino acids were pre-activated with DCC/6-Cl-HOBt (1:1:1) in DMF at room temperature (RT) for 10 min, and the coupling reaction was allowed to proceed for 2–24 h; coupling and deprotection steps were confirmed by the Kaiser test.[44] Synthesized peptides were cleaved with a cocktail containing TFA/water/TIPS/EDT (93/2/2.5/2.5 v/v/v). The reaction was stirred for 8 h at RT, then the resin–peptide was filtered, and the solution was collected. Crude peptides were precipitated and washed by treatment with cold ethyl ether and finally dried at RT. The yield of peptide synthesis cannot be accurately determined due to the process used in this synthesis. In the initial stages, the peptides are developed in the same reactor, and the resin is qualitatively divided when the sequence changes; peptides [Pal], Ahx-[Pal], CH_3CO-Ahx-[Pal], and Biotin-Ahx-[Pal] were obtained from the same reactor, and the resin is qualitatively cleaved when there is a change in the sequence. When the last arginine was incorporated, the resin–peptide was divided to obtain the peptide [Pal]. Subsequently, after the incorporation of Ahx, the

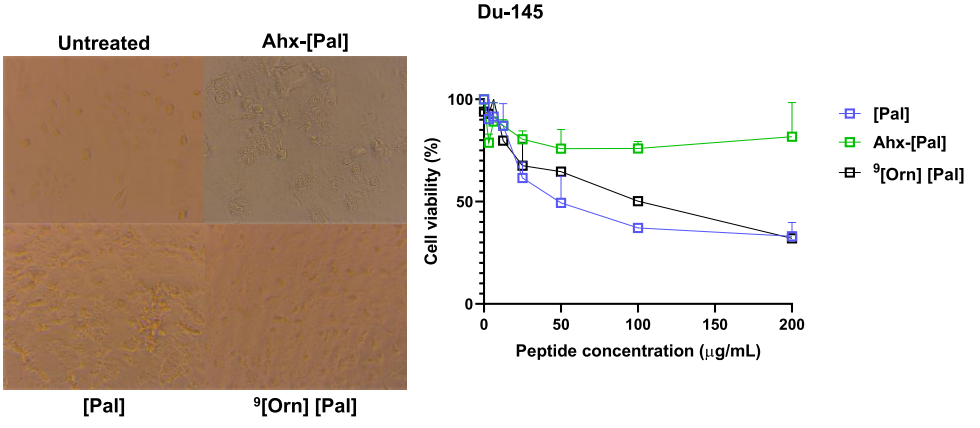

Figure 7. (Left) micrography of Du-145 cells treated with peptides at the maximum peptide concentration (200 μg/mL) using an AxioCam ICc1 camera (scale bar: 100 μm). (Right) MTT assays. Cells treated with peptides (0–200 μg/mL) during 2 h. The data are expressed as the mean ± SE (n = 3).

https://doi.org/10.1021/acsomega.3c03455
ACS Omega 2023, 8, 37948–37957

resin−peptide was divided again to obtain Ahx-[Pal]. The remaining resin−peptide was then divided once more to incorporate either biotin or CH_3CO, resulting in the formation of CH_3CO-Ahx-[Pal] or Biotin-Ahx-[Pal], respectively.

Peptide Purification. The molecules were dissolved in mobile phase A (0,05% TFA in H_2O) and loaded onto solid-phase extraction columns (SUPELCO LC-18 with 2.0 g resin). Solid-phase extraction (SPE) columns were activated prior to use with acetonitrile (0.05% TFA) and equilibrated with water (0.05% TFA). A gradient was used for their elution and the collected fractions were analyzed using reversed-phase high-performance liquid chromatography (RP-HPLC) and, if contained, the pure products were lyophilized.[45]

Peptide Characterization. RP-HPLC was performed on a Merck Chromolith C18 (50 mm × 4.6 mm) column using an Agilent 1200 liquid chromatograph (Omaha, NE) with an ultraviolet−visible (UV−vis) detector (210 nm). For peptide analysis, a linear gradient was applied from 5 to 50% solvent B (0.05% TFA in ACN) in solvent A (0.05% TFA in water) for 8 min at a flow rate of 2.0 mL/min at RT. 10 μL of crude or pure samples were injected with an approximate concentration of 1.0 mg/mL. Expected masses were confirmed using liquid chromatography−mass spectrometry (LC−MS); peptides (10 μg/mL) were analyzed on a Bruker Impact II LC quadrupole time-of-flight (Q-TOF) MS spectrometer equipped with an electrospray ionization (ESI) source operated in positive mode at the conditions: late end offset 500 V, capillary voltage 4500 V, drying temperature 220 °C, and nitrogen flow 8 L/min. Expected mass and chemical structures were drawn using the software Chemdraw Professional 20 (PerkinElmer Informatics, Inc.).

Cell Culture. For Caco-2 and HT-29 cells, the medium used was Dulbecco's modified Eagle's medium (DMEM). For HEK-293, fibroblast, and Vero cell lines, the medium used was Roswell Park Memorial Institute (RPMI-1640) medium. For all cell lines, the medium was supplemented with 10% fetal bovine serum (SFB). All mediums were filtered through a 0.22 μm membrane.

Viability Test by Means of MTT. Cytotoxic assays were performed as previously described.[37] Briefly, 1×10^4 cells per well were seeded and synchronized in 96-well plates for 24 h. The medium was then changed to a peptide solution in the same medium for 2 h at 37 °C. To test cell viability, 10 μL of MTT solution (5 mg/mL) was added to each well and incubated for 4 h at 37 °C, then the medium was removed, 100 μL of dimethyl sulfoxide (DMSO) at 37 °C for 30 min, and absorbance was read on a Bio-Rad 680 microplate reader (570 nm).

Hemolytic Activity. Hemolysis assays were performed as previously described.[35] The blood was donated by healthy volunteers with blood type O^+. 5 mL of peripheral blood in EDTA was centrifuged at 500 rpm, and the erythrocytes were separated and washed 3 times with a 0.9% saline solution. Then, 100 μL of peptide (final concentrations of 200 to 6.2 μg mL^{-1}) was mixed with 100 μL of erythrocytes (2% hematocrit) and incubated at 37 °C for 2 h. It was then centrifuged at 2500 rpm for 5 min, and the absorbance of the supernatant was measured at 450 nm. The controls used were as follows: positive control: distilled water and Tween 20, and negative control: saline solution 0.9%. Hemolytic activity was determined as the concentration of the peptide to cause 10% hemolysis.

***In Silico* Testing.** Molecules were drawn in ChemDraw software, and the SMILES code was generated to analyze it in the freely available ADMETLab 2.0 platform.[26] The structural projection was made using Maestro, Schrödinger, LLC, New York, NY, 2023. The hemolytic effect of [Pal] was assessed by writing the sequence on the HAPPENN platform.[38]

Galleria Mellonella. A toxicity assay was assessed in a Galleria mellonella model as previously described.[46] Briefly, the larvae were obtained from Productos Biológicos Perkins Ltda (Palmira, Valle del Cauca, Colombia). Larvae in the last larval stadium weighing 200−300 mg. Initially, the larvae were rinsed with sterile water. The larvae were inoculated at the last proleg with 10 μL of saline solution or each peptide. The larvae were maintained in Petri dishes (n = 10, per group) and incubated in darkness at 37 °C. The dead larvae were detected by lack of movement. Survival was monitored every 24 h over a period of 10 days.

■ ASSOCIATED CONTENT

Supporting Information

The Supporting Information is available free of charge at https://pubs.acs.org/doi/10.1021/acsomega.3c03455.

HPLC and LC−MS data; graphs illustrating cell viability, and methodological data (PDF)

■ AUTHOR INFORMATION

Corresponding Author

Javier E. García-Castañeda − *Department of Pharmacy, Universidad Nacional de Colombia, Bogotá 111321, Colombia;* orcid.org/0000-0001-6882-4397; Email: jaegarciaca@unal.edu.co

Authors

Karen J. Cárdenas-Martínez − *Department of Pharmacy, Universidad Nacional de Colombia, Bogotá 111321, Colombia;* orcid.org/0000-0002-7266-8769

Andrea C. Barragán-Cárdenas − *Department of Biotechnology, Universidad Nacional de Colombia, Bogotá 111321, Colombia*

Manuela de la Rosa-Arbeláez − *Deparment of Chemistry, Universidad Nacional de Colombia, Bogotá 111321, Colombia*

Claudia M. Parra-Giraldo − *Proteomics and Human Mycosis Unit, Infectious Diseases Research Group, Department of Microbiology, Pontificia Universidad Javeriana, Bogotá 110231, Colombia*

Alejandra Ochoa-Zarzosa − *Multidisciplinary Centre for Studies in Biotechnology, Universidad Michoacana de San Nicolas de Hidalgo, Tarímbaro 58880, México*

Joel E. Lopez-Meza − *Multidisciplinary Centre for Studies in Biotechnology, Universidad Michoacana de San Nicolas de Hidalgo, Tarímbaro 58880, México*

Zuly J. Rivera-Monroy − *Deparment of Chemistry, Universidad Nacional de Colombia, Bogotá 111321, Colombia;* orcid.org/0000-0001-6915-8488

Ricardo Fierro-Medina − *Deparment of Chemistry, Universidad Nacional de Colombia, Bogotá 111321, Colombia*

Complete contact information is available at: https://pubs.acs.org/10.1021/acsomega.3c03455

Author Contributions

Conceptualization: K.J.C.M., C.M.P.G., Z.J.R.M., and J.E.G.C.; investigation: K.J.C.M., A.C.B.C., and M.R.A; funding acquisition: C.M.P.G., Z.J.R.M., and J.E.G.C.; resources: C.M.P.G., Z.J.R.M., J.E.G.C., A.O.Z., J.E.L.M., and R.F.M; writing—original draft preparation: K.J.C.M; and writing—review and editing: Z.J.R.M. and J.E.G.C.

Notes

The authors declare no competing financial interest.

■ ACKNOWLEDGMENTS

This research was conducted with the financial support of COLCIENCIAS—Code 110184466986, contract RC No. 845-2019. K.J.C.M. thanks the Joven Investigator Scholarships—Internships for those selected for the Otto de Greiff National Competition.

■ REFERENCES

(1) Kamb, A.; Wee, S.; Lengauer, C. Why Is Cancer Drug Discovery so Difficult? *Nat. Rev. Drug Discovery* **2007**, *6*, 115−120.
(2) Siegel, R. L.; Miller, K. D.; Wagle, N. S.; Jemal, A. Cancer Statistics, 2023. *Ca-Cancer J. Clin.* **2023**, *73*, 17−48.
(3) Ahnen, D. J.; Wade, S. W.; Jones, W. F.; Sifri, R.; Silveiras, J. M.; Greenamyer, J.; Guiffre, S.; Axilbund, J.; Spiegel, A.; You, Y. N. The Increasing Incidence of Young-Onset Colorectal Cancer: A Call to Action. *Mayo Clin. Proc.* **2014**, *89*, 216−224.
(4) Xi, Y.; Xu, P. Global Colorectal Cancer Burden in 2020 and Projections to 2040. *Transl. Oncol.* **2021**, *14*, No. 101174.
(5) Fabregas, J. C.; Ramnaraign, B.; George, T. J. Clinical Updates for Colon Cancer Care in 2022. *Clin. Colorectal Cancer* **2022**, *21*, 198−203.
(6) Zugazagoitia, J.; Guedes, C.; Ponce, S.; Ferrer, I.; Molina-Pinelo, S.; Paz-Ares, L. Current Challenges in Cancer Treatment. *Clin. Ther.* **2016**, *38*, 1551−1566.
(7) Norouzi, P.; Mirmohammadi, M.; Tehrani, M. H. H. Anticancer Peptides Mechanisms, Simple and Complex. *Chem.-Biol. Interact.* **2022**, *368*, No. 110194.
(8) Chiangjong, W.; Chutipongtanate, S.; Hongeng, S. Anticancer Peptide: Physicochemical Property, Functional Aspect and Trend in Clinical Application (Review). *Int. J. Oncol.* **2020**, *57*, 678−696.
(9) Dobrzyńska, I.; Szachowicz-Petelska, B.; Sulkowski, S.; Figaszewski, Z. Changes in Electric Charge and Phospholipids Composition in Human Colorectal Cancer Cells. *Mol. Cell. Biochem.* **2005**, *276*, 113−119.
(10) Sun, H.; Zhou, Y.; Jiang, H.; Xu, Y. Elucidation of Functional Roles of Sialic Acids in Cancer Migration. *Front. Oncol.* **2020**, *10*, No. 401.
(11) Beloribi-Djefaflia, S.; Vasseur, S.; Guillaumond, F. Lipid Metabolic Reprogramming in Cancer Cells. *Oncogenesis* **2016**, *5*, No. e189.
(12) Butler, L. M.; Perone, Y.; Dehairs, J.; Lupien, L. E.; de Laat, V.; Talebi, A.; Loda, M.; Kinlaw, W. B.; Swinnen, J. V. Lipids and Cancer: Emerging Roles in Pathogenesis, Diagnosis and Therapeutic Intervention. *Adv. Drug Delivery Rev.* **2020**, *159*, 245−293.
(13) Han, X.; Ma, L.; Gu, J.; Wang, D.; Li, J.; Lou, W.; Saiyin, H.; Fu, D. Basal Microvilli Define the Metabolic Capacity and Lethal Phenotype of Pancreatic Cancer. *J. Pathol.* **2021**, *253*, 304−314.
(14) Jafari, A.; Babajani, A.; Sarrami Forooshani, R.; Yazdani, M.; Rezaei-Tavirani, M. Clinical Applications and Anticancer Effects of Antimicrobial Peptides: From Bench to Bedside. *Front. Oncol.* **2022**, *12*, No. 350.
(15) Wang, L.; Wang, N.; Zhang, W.; Cheng, X.; Yan, Z.; Shao, G.; Wang, X.; Wang, R.; Fu, C. Therapeutic Peptides: Current Applications and Future Directions. *Signal Transduction Targeted Ther.* **2022**, *7*, No. 48.
(16) Barragán-Cárdenas, A. C.; Insuasty-Cepeda, D. S.; Cárdenas-Martínez, K. J.; López-Meza, J.; Ochoa-Zarzosa, A.; Umaña-Pérez, A.; Rivera-Monroy, Z. J.; García-Castañeda, J. E. LfcinB-Derived Peptides: Specific and Punctual Change of an Amino Acid in Monomeric and Dimeric Sequences Increase Selective Cytotoxicity in Colon Cancer Cell Lines. *Arabian J. Chem.* **2022**, *15*, No. 103998.
(17) Barragán-Cárdenas, A.; Urrea-Pelayo, M.; Niño-Ramírez, V. A.; Umaña-Pérez, A.; Vernot, J. P.; Parra-Giraldo, C. M.; Fierro-Medina, R.; Rivera-Monroy, Z.; García-Castañeda, J. Selective Cytotoxic Effect against the MDA-MB-468 Breast Cancer Cell Line of the Antibacterial Palindromic Peptide Derived from Bovine Lactoferricin. *RSC Adv.* **2020**, *10*, 17593−17601.
(18) Cárdenas-Martínez, K. J.; Grueso-Mariaca, D.; Vargas-Casanova, Y.; Bonilla-Velásquez, L.; Estupiñán, S. M.; Parra-Giraldo, C. M.; Leal, A. L.; Rivera-Monroy, Z. J.; García-Castañeda, J. E. Effects of Substituting Arginine by Lysine in Bovine Lactoferricin Derived Peptides: Pursuing Production Lower Costs, Lower Hemolysis, and Sustained Antimicrobial Activity. *Int. J. Pept. Res. Ther.* **2021**, *27*, 1751−1762.
(19) Barragán-Cárdenas, A. C.; Insuasty-Cepeda, D. S.; Vargas-Casanova, Y.; López-Meza, J. E.; Parra-Giraldo, C. M.; Fierro-Medina, R.; Rivera-Monroy, Z. J.; García-Castañeda, J. E. Changes in Length and Positive Charge of Palindromic Sequence RWQWRWQWR Enhance Cytotoxic Activity against Breast Cancer Cell Lines. *ACS Omega* **2023**, *8*, 2712−2722.
(20) Huang, Y.; Feng, Q.; Yan, Q.; Hao, X.; Chen, Y. Alpha-Helical Cationic Anticancer Peptides: A Promising Candidate for Novel Anticancer Drugs. *Mini-Rev. Med. Chem.* **2015**, *15*, 73−81.
(21) Hadianamrei, R.; Tomeh, M. A.; Brown, S.; Wang, J.; Zhao, X. Rationally Designed Short Cationic α-Helical Peptides with Selective Anticancer Activity. *J. Colloid Interface Sci.* **2022**, *607*, 488−501.
(22) Mura, M.; Wang, J.; Zhou, Y.; Pinna, M.; Zvelindovsky, A. V.; Dennison, S. R.; Phoenix, D. A. The Effect of Amidation on the Behaviour of Antimicrobial Peptides. *Eur. Biophys. J.* **2016**, *45*, 195−207.
(23) Chan, D. I.; Prenner, E. J.; Vogel, H. J. Tryptophan- and Arginine-Rich Antimicrobial Peptides: Structures and Mechanisms of Action. *Biochim. Biophys. Acta, Biomembr.* **2006**, *1758*, 1184−1202.
(24) Shen, Y.; Maupetit, J.; Derreumaux, P.; Tufféry, P. Improved PEP-FOLD Approach for Peptide and Miniprotein Structure Prediction. *J. Chem. Theory Comput.* **2014**, *10*, 4745−4758.
(25) Thevenet, P.; Shen, Y.; Maupetit, J.; Guyon, F.; Derreumaux, P.; Tuffery, P. PEP-FOLD: An Updated de Novo Structure Prediction Server for Both Linear and Disulfide Bonded Cyclic Peptides. *Nucleic Acids Res.* **2012**, *40*, W288−W293.
(26) Xiong, G.; Wu, Z.; Yi, J.; Fu, L.; Yang, Z.; Hsieh, C.; Yin, M.; Zeng, X.; Wu, C.; Lu, A.; Chen, X.; Hou, T.; Cao, D. ADMETlab 2.0: An Integrated Online Platform for Accurate and Comprehensive Predictions of ADMET Properties. *Nucleic Acids Res.* **2021**, *49*, W5−W14.
(27) Ertl, P.; Schuffenhauer, A. Estimation of Synthetic Accessibility Score of Drug-like Molecules Based on Molecular Complexity and Fragment Contributions. *J. Cheminf.* **2009**, *1*, No. 8.
(28) Vinothini, K.; Rajendran, N. K.; Munusamy, M. A.; Alarfaj, A. A.; Rajan, M. Development of Biotin Molecule Targeted Cancer Cell Drug Delivery of Doxorubicin Loaded κ-Carrageenan Grafted Graphene Oxide Nanocarrier. *Mater. Sci. Eng.: C* **2019**, *100*, 676−687.
(29) Wu, Y. P.; Chew, C. Y.; Li, T. N.; Chung, T. H.; Chang, E. H.; Lam, C. H.; Tan, K. T. Target-Activated Streptavidin−Biotin Controlled Binding Probe. *Chem. Sci.* **2018**, *9*, 770−776.
(30) Dong, J.; Wang, N. N.; Yao, Z. J.; Zhang, L.; Cheng, Y.; Ouyang, D.; Lu, A. P.; Cao, D. S. Admetlab: A Platform for Systematic ADMET Evaluation Based on a Comprehensively Collected ADMET Database. *J. Cheminf.* **2018**, *10*, No. 29.
(31) Markowska, A.; Markowski, A. R.; Jarocka-Karpowicz, I. The Importance of 6-Aminohexanoic Acid as a Hydrophobic, Flexible Structural Element. *Int. J. Mol. Sci.* **2021**, *22*, No. 12122.
(32) Yang, Y.; Zhang, H.; Wanyan, Y.; Liu, K.; Lv, T.; Li, M.; Chen, Y. Effect of Hydrophobicity on the Anticancer Activity of Fatty-Acyl-Conjugated CM4 in Breast Cancer Cells. *ACS Omega* **2020**, *5*, 21513−21523.

https://doi.org/10.1021/acsomega.3c03455
ACS Omega 2023, 8, 37948−37957

(33) Huang, Y.-b.; Wang, X.-f.; Wang, H.-y.; Liu, Y.; Chen, Y. Studies on Mechanism of Action of Anticancer Peptides by Modulation of Hydrophobicity within a Defined Structural Framework. *Mol. Cancer Ther.* **2011**, *10*, 416−426.
(34) Yang, S. T.; Shin, S. Y.; Lee, C. W.; Kim, Y. C.; Hahm, K. S.; Kim, J. Il. Selective Cytotoxicity Following Arg-to-Lys Substitution in Tritrpticin Adopting a Unique Amphipathic Turn Structure. *FEBS Lett.* **2003**, *540*, 229−233.
(35) Oba, M.; Nagano, Y.; Kato, T.; Tanaka, M. Secondary Structures and Cell-Penetrating Abilities of Arginine-Rich Peptide Foldamers. *Sci. Rep.* **2019**, *9*, No. 1349.
(36) Modimola, M. S.; Green, E.; Njobeh, P.; Senabe, J.; Fouche, G.; McGaw, L.; Nkadimeng, S. M.; Mathiba, K.; Mthombeni, J. Investigating the Toxicity of Compounds Yielded by Staphylococci on Vero Cells. *Toxins* **2022**, *14*, No. 712.
(37) Freire, P. F.; Labrador, V.; Martín, J. M. P.; Hazen, M. J. Cytotoxic Effects in Mammalian Vero Cells Exposed to Pentachlorophenol. *Toxicology* **2005**, *210*, 37−44.
(38) Timmons, P. B.; Hewage, C. M. HAPPENN is a Novel Tool for Hemolytic Activity Prediction for Therapeutic Peptides Which Employs Neural Networks. *Sci. Rep.* **2020**, *10*, No. 10869.
(39) Li, J.; Yanagisawa, K.; Yoshikawa, Y.; Ohue, M.; Akiyama, Y. Plasma Protein Binding Prediction Focusing on Residue-Level Features and Circularity of Cyclic Peptides by Deep Learning. *Bioinformatics* **2022**, *38*, 1110−1117.
(40) McCann, M.; Santos, A. L. S.; da Silva, B. A.; Romanos, M. T. V.; Pyrrho, A. S.; Devereux, M.; Kavanagh, K.; Fichtner, I.; Kellett, A. In Vitro and in Vivo Studies into the Biological Activities of 1,10-Phenanthroline, 1,10-Phenanthroline-5,6-Dione and Its Copper(Ii) and Silver(i) Complexes. *Toxicol. Res.* **2012**, *1*, 47−54.
(41) Perše, M. Cisplatin Mouse Models: Treatment, Toxicity and Translatability. *Biomedicines* **2021**, *9*, No. 1406.
(42) Berman, J. R.; Nunnemann, R. G.; Broshears, J. R.; Berman, I. R. Sigmoid Colon Carcinoma Metastatic to Prostate. *Urology* **1993**, *41*, 150−151.
(43) Kang, A.; Lee, J. H.; Lin, E.; Westerhoff, M. Metastatic Colon Carcinoma to the Prostate Gland. *J. Comput. Assist. Tomogr.* **2013**, *37*, 463−465.
(44) Kaiser, E.; Colescott, R. L.; Bossinger, C. D.; Cook, P. I. Color Test for Detection of Free Terminal Amino Groups in the Solid-Phase Synthesis of Peptides. *Anal. Biochem.* **1970**, *34*, 595−598.
(45) Cepeda, D. I.; Castañeda, H. P.; Mayor, A. R.; Castañeda, J. G.; Villamil, M. M.; Medina, R. F.; Monroy, Z. R. Synthetic Peptide Purification via Solid-Phase Extraction with Gradient Elution: A Simple, Economical, Fast, and Efficient Methodology. *Molecules* **2019**, *24*, No. 1215.
(46) Bravo-Chaucanés, C. P.; Vargas-Casanova, Y.; Chitiva-Chitiva, L. C.; Ceballos-Garzon, A.; Modesti-Costa, G.; Parra-Giraldo, C. M. Evaluation of Anti-Candida Potential of Piper Nigrum Extract in Inhibiting Growth, Yeast-Hyphal Transition, Virulent Enzymes, and Biofilm Formation. *J. Fungi* **2022**, *8*, No. 784.

https://doi.org/10.1021/acsomega.3c03455
ACS Omega 2023, 8, 37948−37957